Spectrochimica Acta Part A: Molecular and Biomolecular Spectroscopy 108 (2013) 319–328

Contents lists available at SciVerse ScienceDirect

Spectrochimica Acta Part A: Molecular and Biomolecular Spectroscopy

journal homepage: www.elsevier.com/locate/saa

Dicoumarol complexes of Cu(II) based on 1,10-phenanthroline: Synthesis, X-ray diffraction studies, thermal behavior and biological evaluation

Hitesh R. Dholariya, Ketan S. Patel, Jiten C. Patel, Kanuprasad D. Patel *

V.P. & R.P.T.P. Science College, Sardar Patel University, Vallabh Vidyanagar 388 120, Gujarat, India

HIGHLIGHTS

- Mixed-ligand Cu(II) complexes based on dicoumarol with 1,10-phenanthroline.
- Octahedral geometry was confirmed using electronic spectra, X-ray diffraction studies and magnetic measurement.
- Measurements of kinetic parameters using Freeman–Carroll method.
- Antioxidant, anti-tubercular and antimicrobial studies of complexes.

GRAPHICAL ABSTRACT

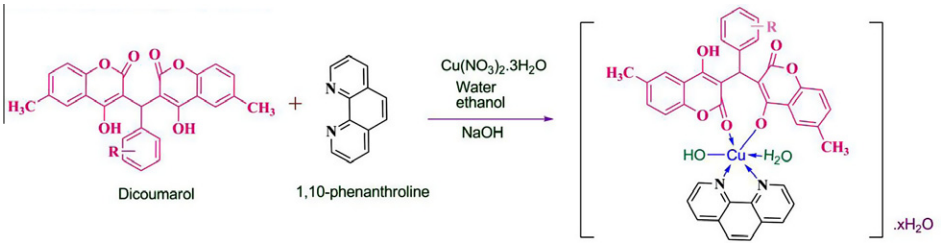

ARTICLE INFO

Article history:
Received 29 June 2012
Received in revised form 30 August 2012
Accepted 8 September 2012
Available online 12 October 2012

Keywords:
Dicoumarol derivative
1, 10-Phenanthroline
X-ray diffraction study
Antimicrobial
Antioxidant
Anti-tubercular

ABSTRACT

A series of Cu(II) complexes containing dicoumarol derivatives and 1, 10-phenanthroline have been synthesized. Structural and spectroscopic properties of ligands were studied on the basis of mass spectra, NMR (^{1}H and ^{13}C) spectra, FT-IR spectrophotometry and elemental analysis, while physico-chemical, spectroscopic and thermal properties of mixed ligand complexes have been studied on the basis of infrared spectra, mass spectra, electronic spectra, powder X-ray diffraction, elemental analysis and thermogravimetric analysis. X-ray diffraction study suggested the suitable octahedral geometry for hexa-coordinated state. The kinetic parameters such as order of reaction (n), energy of activation (E_a), entropy (S^*), pre-exponential factor (A), enthalpy (H^*) and Gibbs free energy (G^*) have been calculated using Freeman–Carroll method. Ferric-reducing antioxidant power (FRAP) of all complexes were measured. All the compounds were screened for their antibacterial activity against *Escherichia coli*, *Pseudomonas aeruginosa*, *Streptococcus pyogenes* and *Bacillus subtilis*, while antifungal activity against *Candida albicans* and *Aspergillus niger* have been carried out. Also compounds against *Mycobacterium tuberculosis* shows clear enhancement in the anti-tubercular activity upon copper complexation.

Introduction

4-Hydroxycoumarin derivatives have a lot of applications as drugs with several type of pharmacological agents possessing anti-coagulant, spasmolytic, bacteriostatic, potential anti-HIV, anti-fungal and herbicides activity among others. Some coumarin derivatives are known for their *in vitro* antibiotic and antifungal activities, furthermore some of the investigated compounds show low toxicity and dose dependent anticoagulant activity *in vivo*. They are also extensively used as analytical reagents [1,2]. The antitumor activities of coumarin and its known metabolite coumarin derivatives were tested in several human tumor cell lines by Steffen et al. [3]. Many coumarin derivatives have been well-known from natural sources, especially green plants. The very long association of plant coumarins with various animal species and other organisms throughout progress may account for the surprising range of biochemical and pharmacological activities. Coumarins have important effects as enzyme inhibitors [4–6] and they are precursors of toxic substances. In addition, these compounds are involved in the actions of plant growth hormones and growth regulators, Control of respiration, photosynthesis and defense against infection. The coumarins have been recognized to

* Corresponding author. Tel.: +91 2692 230011; fax: +91 2692 235207.
E-mail addresses: hitesh.msc123@gmail.com (H.R. Dholariya), drkdpatel64@yahoo.co.in (K.D. Patel).

1386-1425/$ - see front matter © 2012 Elsevier B.V. All rights reserved.
http://dx.doi.org/10.1016/j.saa.2012.09.096

possess anti-inflammatory, antioxidant, antiallergic, hepatoprotective, antithrombotic, antiviral and anticarcinogenic activities [7]. Recently, an area of coumarin chemistry is increasing that concerns important biologically active metal complexes of coumarin-based ligands. In general, coordination of metal ions to therapeutic agents improves their efficacy and accelerates bioactivity. In this context, a broad array of medicinal applications of metal complexes has been investigated [8–13].

1,10-Phenanthroline(Ph) is well-known chelating bidentate ligand for transition metal ions which played an important role in many fields such as coordination chemistry [14,15], in agreement with the electron-deficient characteristics of the hetero aromatic rings and to the consequent lower σ-donor ability of its nitrogen atoms [16], in spite of the low σ-donor ability of the hetero aromatic nitrogen atoms, the stability of these complexes is somewhat higher mainly due to the hydrophobic nature of Ph and to the consequent larger desolvation of metal cations upon complex formation [17,18]. In recent years, the study of Cu—Ph complexes has become progressively more important due to their antimicrobial and antioxidant properties [19–21].

In our previous reports, we have mentioned a series of coumarin derivatives and its transition metal complexes [22–25]. Herein we report the synthesis, antimicrobial, antioxidation and antitubercular activities of Cu(II) mixed ligand complexes using 1,10-phenanthrolin with coumarin derivatives. We describe here characterization, powder X-ray diffraction study and spectroscopic features of new mixed ligand Cu(II) complexes. The thermal behavior of these complexes has been investigated by using thermogravimetric (TG) analysis. Thermogravimetry is a process in which a substance is decomposed in the presence of heat, which causes bonds of the molecules to be broken [26,27]. Kinetic parameters like order of reaction (n), activation energy (E_a), entropy change (S^*), enthalpy change (H^*), free energy change (G^*) and pre-exponential factor (A) are measured out using kinetic studies of thermal decomposition reactions.

Experimental

Materials, instruments and methods

Chemicals were purchased from the following commercial sources: Spectrochem Pvt. Ltd., Mumbai, E. Merck Pvt. Ltd., Mumbai, s.d. fine-chem Ltd., Mumbai and used as received. All solvents of analytical grade were distilled, purified and dried using appropriate methods [28]. All reactions were monitored by thin-layer chromatography (TLC on aluminium plates coated with silica gel 60 F_{254}, 0.25 mm thickness, Merck) and detection of the components were carried out under UV light or explored in iodine chamber. The metal nitrates were used in hydrated form. Elemental analysis was performed on elemental analyzer PerkinElmer, USA 2400-II CHN. Analyses of metal ions were carried out by the dissolution of the solid complexes in hot concentrated nitric acid, further diluting with distilled water and filtered to remove the precipitated organic ligands. Remaining solution was neutralized with ammonia solution and the metal ions were titrated against EDTA. Melting points were measured using open capillary. Infrared spectra were recorded in the region of 4000–400 cm^{-1} on Shimadzu FTIR 8401 spectrophotometer. All infrared spectra were run as potassium bromide pellets. ^1H and ^{13}C NMR measurements were carried out on Advance-II 400 MHz Bruker NMR spectrometer. Chemical shifts were measured with respect to TMS as internal standard and DMSO-d_6 used as solvent. The Mass spectra were recorded on Thermo Scientific, USA. Electronic spectra were recorded on a LAMBDA 19 UV/VIS/NIR in the region of 200–1200 nm. Thermogravimetric scans were run on a model Diamond TG/DTA, PerkinElmer, USA. The analysis carried out under a nitrogen atmosphere at a heating rate of 20 °C/min from 30 °C to 840 °C. Effective magnetic susceptibility measurement were calculated by the Gouy's method using mercury tetrathiocyanato cobaltate (II) as a calibrant ($\chi = 16.44 \times 10^{-6}$ c.g.s. units at 20 °C). Molar susceptibility was corrected using Pascal's constant [29].

Crystallographic analysis

X-ray diffraction intensities were carried out with ±0.0025 accuracy using XRD Diffractometer (powder), Xpert MPD, Philips, Holland equipped with 2 kW power and Cu target X-ray tube used as a source of wavelength 1.542 Å, while the data were accumulate using JCPDF database. The detector used in the system was Xe-filled counterate and 2° θ measurement range of the instrument is 3–136°. The system contains goniometer was operated on vertical and horizontal mode with θ–θ and θ–2θ position respectively with radius 130–230 mm.

Preparation of ligands

4-Hydroxy-6-methyl-2H-chromen-2-one: 6-methyl-4-hydroxycoumarin was synthesized as reported method [30].

Synthesis of ligands (HL1–HL6)

General procedure for synthesis of the ligands **(HL)** is shown in Scheme 1. The ligands were characterized using elemental analysis, FT-IR, Mass spectra and NMR (^1H and ^{13}C) spectroscopy.

3, 3′-(Phenylmethylene)bis(4-hydroxy-6-methyl-2H-chromen-2-one-(HL1)

An ethanolic solution (25 mL) of 6-methyl-4-hydroxycoumarin (0.02 mol) was heated in water bath for 2 h, to obtain a clear solution. Ethanolic solution of benzaldehyde (0.01 mol) (25 mL) was added in reaction mass and refluxed in presence of catalytic amount of H_2SO_4 for 18 h. and the progress of the reaction was monitored by TLC using mobile phase Ethyl acetate:Haxane (6:4). After the completion of reaction, the reaction mixture was cooled to room temperature. The product obtained was separated out and were recrystallized from ethanol. Yield, 65%; m.p. 235 °C. Anal. Calcd. for $C_{27}H_{20}O_6$: C, 73.41, H, 4.79. calculated: C, 73.63, H, 4.58; FT-IR (KBr cm^{-1}): 3180, 3050 ν(—OH/H_2O) cm^{-1}, 1663 ν(C=O) cm^{-1}, 1623, 1574 ν(C=C) cm^{-1}, 1179, 1125, 1089, 820, 790, 744 ν(C—O) cm^{-1}, 2923(asym), 2738(sym) $\nu(CH_3)$ cm^{-1}, 1436(asym), 1356(sym) $\delta(CH_3)$ cm^{-1}. ^1H NMR (DMSO-d_6 400 MHz): δ: 2.376 (6H, s, —CH_3), 6.485 (^1H, Aliphatic), 7.167–7.873 (11H, m, Aromatic proton), 10.156 (—OH phenolic); ^{13}C NMR (DMSO-d_6 100 MHz): δ: 21.30 (C-24, 25), 35.67 (C-9), 103.54 (C-3, 18), 115.57, 117.22, 123.91, 127.08, 127.83, 128.35,132.19, 132.65, 141.24 (8C, Ar–C), 150.43 (C-8a, 23a), 164.67 (C-2, 17), 165.55 (C-4, 19); ESI-MS (m/z): 440.7.

3, 3′-((3-Hydroxyphenyl)methylene)bis(4-hydroxy-6-methyl-2H-chromen-2-one(HL2)

HL2 was synthesized by the same method used for HL1 by using 3-hydroxybenzaldehyde as a substitute of benzaldehyde. Yield, 72%; m.p. 214 °C. Anal. Calcd. for $C_{27}H_{20}O_7$: C, 71.24, H, 4.20. calculated: C, 71.05, H, 4.42; FT-IR (KBr cm^{-1}): 3135, 3054 ν(—OH/H_2O) cm^{-1}, 1666 ν(C=O) cm^{-1}, 1624,1576 ν(C=C) cm^{-1}, 1152, 1125, 1094, 819, 792, 776 ν(C—O) cm^{-1}, 2926(asym), 2861(sym) $\nu(CH_3)$ cm^{-1}, 1449(asym), 1354(sym) $\delta(CH_3)$ cm^{-1}. ^1H NMR (DMSO-d_6 400 MHz): δ: 2.365 (6H, s, —CH_3), 6.267 (1H, Aliphatic), 6.519–7.701 (10H, m, Aromatic proton), 9.231, 10.253 (—OH phenolic); ^{13}C NMR (DMSO-d_6 100 MHz): δ: 21.55 (C-24, 25), 35.79 (C-9), 103.96 (C-3, 18), 112.50 , 113.53, 115.67, 117.32, 117.63, 123.55,

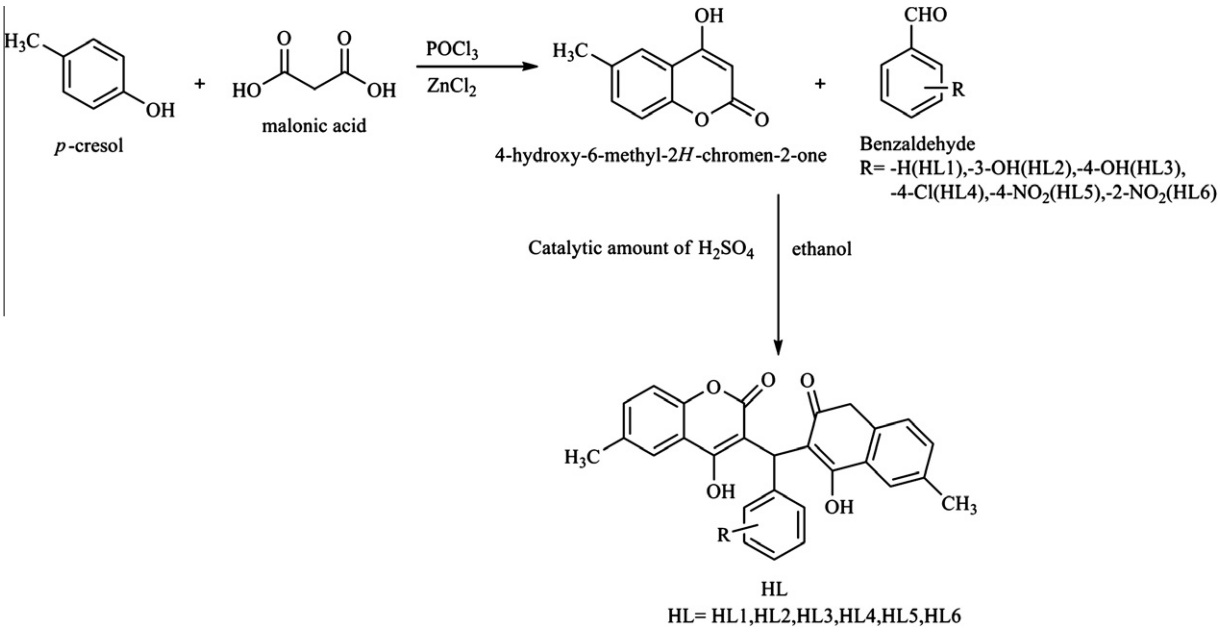

Scheme 1. General procedure for synthesis of ligands (HL).

128.88, 132.63, 132.86, 141.47 (10C, Ar–C), 150.28 (C-8a, 23a), 157.17 (C-12), 164.95 (C-2, 17), 165.34 (C-4, 19); ESI-MS (*m/z*): 456.4.

3, 3′-((4-Hydroxyphenyl)methylene)bis(4-hydroxy-6-methyl-2H-chromen-2-one(HL3)

HL3 was synthesized by the same method used for HL1 by using 4-hydroxybenzaldehyde as a substitute of benzaldehyde. Yield, 68%; m.p. 221 °C. Anal. Calcd. for $C_{27}H_{20}O_7$: C, 71.32, H, 4.63. calculated: C, 71.05, H, 4.42; FT-IR (KBr cm^{-1}): 3170,3045 *v*(—OH/H_2O) cm^{-1}, 1665 *v*(C=O) cm^{-1}, 1623,1575 *v*(C=C) cm^{-1}, 1165, 1123, 1087, 815, 787, 745 *v*(C—O) cm^{-1}, 2924(asym), 2840(sym) *v*(CH_3) cm^{-1}, 1438(asym), 1352(sym) *δ*(CH_3) cm^{-1}. ^{1}H NMR (DMSO-d_6 400 MHz): *δ*: 2.364 (6H, s, —CH_3), 6.405 (1H, Aliphatic), 7.113–7.815 (10H, m, Aromatic proton), 9.311, 10.156 (—OH phenolic); ^{13}C NMR (DMSO-d_6 100 MHz): *δ*: 21.30 (C-24, 25), 35.67 (C-9), 103.54 (C-3, 18), 112.32 , 115.87, 117.82, 123.48, 128.36, 132.23, 132.92, 134.15, (8C, Ar–C), 150.46 (C-8a, 23a), 158.75 (C-13), 164.52 (C-2, 17), 165.44 (C-4, 19); ESI-MS (*m/z*): 456.8.

3, 3′-((4-Chlorophenyl)methylene)bis(4-hydroxy-6-methyl-2H-chromen-2-one(HL4)

HL4 was synthesized by the same method used for HL1 by using 4-chlorobenzaldehyde as a substitute of benzaldehyde. Yield, 70%; m.p. 265 °C. Anal. Calcd. for $C_{27}H_{19}ClO_6$: C, 68.48, H, 4.24. calculated: C, 68.29, H, 4.03; FT-IR (KBr cm^{-1}): 3195,3052 *v*(—OH/H_2O) cm^{-1}, 1661 *v*(C=O) cm^{-1}, 1625,1574 *v*(C=C) cm^{-1}, 1201, 1124, 1086, 816, 786, 711 *v*(C—O) cm^{-1}, 2926(asym), 2731(sym) *v*(CH_3) cm^{-1}, 1440(asym), 1346(sym) *δ*(CH_3) cm^{-1}. ^{1}H NMR (DMSO-d_6 400 MHz): *δ*: 2.366 (6H, s, —CH_3), 6.389 (^{1}H, Aliphatic), 7.171–8.142 (10H, m, Aromatic proton), 10.044 (—OH phenolic); ^{13}C NMR (DMSO-d_6 100 MHz): *δ*: 21.35 (C-24, 25), 36.04 (C-9), 103.56 (C-3, 18), 115.25, 118.02, 122.12, 125.48, 128.63, 132. 07, 132.51, 135.02, 141.32 (9C, Ar–C), 150.14 (C-8a, 23a), 165.06 (C-2, 17), 165.82 (C-4, 19); ESI-MS (*m/z*): 474.3, 476.4(M + H^+).

3, 3′-((4-Nitrophenyl)methylene)bis(4-hydroxy-6-methyl-2H-chromen-2-one(HL5)

HL5 was synthesized by the same method used for HL1 by using 4-nitrobenzaldehyde as a substitute of benzaldehyde. Yield, 66%; m.p. 282 °C. Anal. Calcd. for $C_{27}H_{19}NO_8$: C, 66.78, H, 4.12, N, 2.67. calculated: C, 66.80, H, 3.95, N, 2.89; FT-IR (KBr cm^{-1}): 3140, 3025 *v*(—OH/H_2O) cm^{-1}, 1664 *v*(C=O) cm^{-1}, 1621 ,1573 *v*(C=C) cm^{-1}, 1150, 1122, 1088, 815, 785, 735 *v*(C—O) cm^{-1}, 2920(asym), 2756(sym) *v*(CH_3) cm^{-1}, 1442(asym), 1340(sym) *δ*(CH_3) cm^{-1}. ^{1}H NMR (DMSO-d_6 400 MHz): *δ*: 2.382 (6H, s, —CH_3), 6.353 (^{1}H, Aliphatic), 7.128–8.234 (10H, m, Aromatic proton), 10.412 (—OH phenolic); ^{13}C NMR (DMSO-d_6 100 MHz): *δ*: 21.73 (C-24, 25), 35.82 (C-9), 103.58 (C-3, 18), 115.39, 117.65, 121.43, 123.21, 128.37, 132. 51, 132.90, 136.23, 141.48 (9C, Ar–C), 150.64 (C-8a, 23a), 164.80 (C-2, 17), 165.55 (C-4, 19); ESI-MS (*m/z*): 485.2.

3, 3′-((2-Nitrophenyl)methylene)bis(4-hydroxy-6-methyl-2H-chromen-2-one(HL6)

HL6 was synthesized by the same method used for HL1 by using 2-nitrobenzaldehyde as a substitute of benzaldehyde. Yield, 62%; m.p. 275 °C. Anal. Calcd. for $C_{27}H_{19}NO_8$: C, 66.91, H, 4.24, N, 2.74. calculated: C, 66.80, H, 3.95, N, 2.89; FT-IR (KBr cm^{-1}): 3150.3035 *v*(m, —OH/H_2O) cm^{-1}, 1660 *v*(C=O) cm^{-1}, 1623, 1574 *v*(C=C) cm^{-1}, 1162, 1120, 1079, 817, 787, 740 *v*(C—O) cm^{-1}, 2923(asym), 2746(sym) *v*(CH_3) cm^{-1}, 1437(asym), 1350(sym) *δ*(CH_3) cm^{-1}. ^{1}H NMR (DMSO-d_6 400 MHz): *δ*: 2.360 (6H, s, —CH_3), 6.377 (^{1}H, Aliphatic), 7.184–8.364 (10H, m, Aromatic proton), 10.630 (—OH phenolic); ^{13}C NMR (DMSO-d_6 100 MHz): *δ*: 21.47 (C-24, 25), 35.37 (C-9), 103.25 (C-3, 18), 116.40, 117.26, 123.36, 123.85, 128.57, 131. 05, 132.14, 132.62, 132.93, 141.28, 148.11 (11C, Ar–C), 150.32 (C-8a, 23a), 164.63 (C-2, 17), 165.72 (C-4, 19); ESI-MS (*m/z*): 485.8.

Synthesis of metal complexes

All these complexes **HPC1–HPC6** was synthesized according to same procedure as **HPC**, their analytical and physiochemical parameters are summarized in Table 1, while general synthetic route of complexes **(HPC)** shown in Scheme 2.

The Dicoumarol derivatives (0.01 mol) was dissolved in water (25 mL). To that aqueous solution of $Cu(NO_3)_2{\cdot}3H_2O$ (0.01 mol, 25 mL) was gradually added, followed by ethanolic solution of 1,10-phenthroline (0.01 mol, 25 mL). The pH was adjusted to 4.5–6.0 with diluted NaOH solution. Further the mixture was

heated under reflux for 3–5 h and then heated over a steam bath to evaporate up to half of the volume. The reaction mixture was kept overnight at room temperature. A fine amorphous powder was obtained was filtered and dried in air. The physiological and analytical data of the synthesized complexes are listed in Table 1. The complexes comprise high melting points (above 300 °C) and insoluble in common organic solvents and partially soluble in DMSO.

Pharmacology

Antimicrobial assay

Antimicrobial activities of the compounds were tested against the following test microorganisms (all ATCC cultures were collected from Bangalore and tested against above mentioned known drugs): bacteria (*Bacillus subtilis* ATCC11774, *Streptococcus pyogenes* ATCC12384, *Escherichia coli* ATCC25922, *Pseudomonas aeruginosa* ATCC25619) and fungi (*Candida albicans* ATCC66027, *Aspergillus niger* ATCC64958), compared to standard drugs Ciprofloxacin and Norfloxacin (antibacterial), Flucanazole and Nystatin (antifungal) as standard drugs. Bioactivities of the compounds were carried out using Kirby–Bauer disk diffusion method according to the guidelines of Clinical and Laboratory Standards Institute (CLSI) [31]. The Minimum inhibition concentration (MIC) screening data are shown in Table 2. The standard solutions of antibacterial drugs (Ciprofloxacin, Norfloxacin) and antifungal drugs (Flucanazole, Nystatin) were prepared in DMSO. The calculated standard deviation for any result was not more than ±1.0 mm. In this method, antibiotics are impregnated onto paper disks and then placed on a seeded Mueller–Hinton agar plate using a mechanical dispenser or sterile forceps. The plate is then incubated for 16–18 h at 37 °C and the diameter of the zone of inhibition around the disk is measured to the nearest millimeter. The solution of all newly synthesized compounds and standard drugs were prepared at 600, 400, 200, 100, 70, 40, 20 μg/mL concentrations, at 100, 80, 60, 40, 35, 30, 20, 15, 10, 5, 2, 1 μg/mL concentrations in the wells of microplates by diluting in MHB, respectively. The lowest concentration of the compound that completely inhibits macroscopic growth was determined and minimum inhibitory concentrations (MICs) are reported in Table 2.

Method of antioxidant assay

Ferric reducing antioxidant power (FRAP) was measured by a modified method [32]. The antioxidant potentials of the compounds were estimated as their power to reduce the TPTZ–Fe(III) complex to TPTZ–Fe(II) complex, The total antioxidant capacity of biological samples, but we tried the FRAP assay, The method is simple, fast and reproducible results can be obtained. The results are expressed as ascorbic equivalent (mmol/100 g of dried compound).

Preparation of solution:

(a) Acetate buffer, 300 mM pH 3.6 (3.1 g sodium acetate trihydrate and 16 mL conc. acetic acid per L of buffer solution).
(b) 10 mM 2,4,6-tripyridyl-s-triazine (TPTZ) (MW 312.34) in 40 mM HCl.
(c) 20 mM $FeCl_3{\cdot}6H_2O$ (MW 270.30) in distilled water (DW).
(d) 1 mM of ascorbic acid (MW 176.13 g/mol) dissolved in 100 mL DW.

FRAP working solution: Mix the above prepared (a–c) solutions in the ratio of 10:1:1 respectively. A mixture of 40.0 μL, 0.5 mM sample solution and 1.2 mL FRAP reagent was incubated at 37 °C for 15 min. The working solution must be always freshly prepared. The ascorbic acid was used as a standard antioxidant compound. The absorbance of the reaction mixture was measured at 593 nm against a blank containing DMF (400 μL) instead of the sample. The antioxidant activities results were expressed as ascorbic equivalent (mmol/100 g of dried compound).

The FRAP Value can be calculated by following equation:

$$\text{Ascorbic acid concentration(mM/100 g of sample)} = \frac{\Delta A593\text{ nm of test sample}}{\Delta A593\text{ nm of standard}} \times \frac{\text{standard (mm)}}{\text{sample (mg)}} \times 100$$

In vitro evaluation of anti-tuberculosis activity

An anti-tuberculosis activity (MICs) of the title compounds were determined and interpreted for *Mycobacterium tuberculosis* H37Rv according to the procedure of approved micro-dilution reference method of antimicrobial susceptibility testing [33–35]. Compounds were taken at concentrations of 100, 50, 25, 12.5, 6.25 and 3.125 μg/mL in DMSO, 1.0 mL of each concentration was used for the study. To this, 9.0 mL of Lowenstein–Jensen medium was added. A sweep from *M. tuberculosis* H37Rv strain culture was discharged with the help of nichrome wire loop with a 3 mm external diameter into a vial containing 4 mL of sterile distilled water. The vial was shaken for 5 min. Then using nichrome wire loop suspension was inoculated on the surface of each of Lowenstein–Jensen medium containing the test compounds. Further test media was incubated for 28 days at 37 °C. Readings were seen after 28 days of incubation. The appearance of turbidity was considered as bacterial growth and indicates resistance to the compound. Test compounds were compared to reference drugs Isoniazid, Ethambutol and Streptomycin. Lowenstein–Jensen medium containing standard drugs was inoculated with *M. tuberculosis* H37Rv strain. Anti-tubercular activity test was run in triplicate and the deviation for any triplicate results was not more than ±1% to 5% and results are summarized in (Table 3).

Results and discussion

The properties of Cu(II) complexes with coumarin derivatives were studied. The synthesized compounds were explained by elemental analysis, infrared spectra, electronic spectra, mass spectroscopy, X-ray diffraction study, thermal methods, magnetic and kinetic measurements. Further antimicrobial, antioxidant and anti-tuberculosis activities of same compounds were carried out.

Table 1
Analytical and physiochemical parameters of synthesized compounds.

Compounds/empirical formula	Elemental analyses, % found (required)				m.p. (°C)	Yield (%)	Molecular mass	μ_{eff} B.M.
	C	H	N	Cu(II)				
$C_{39}H_{32}CuN_2O_9$/(HPC1)	63.44(63.62)	4.17(4.38)	3.98(3.81)	8.39(8.63)	>350	78	717.26	1.84
$C_{39}H_{34}CuN_2O_{11}$/(HPC2)	60.63(60.81)	4.22(4.45)	3.86(3.64)	8.03(8.25)	>350	70	733.24	1.82
$C_{39}H_{32}CuN_2O_{10/}$(HPC3)	62.45(62.27)	4.05(4.29)	3.93(3.72)	8.61(8.45)	>350	72	733.56	1.91
$C_{39}H_{31}ClCuN_2O_9$/(HPC4)	60.57(60.78)	4.20(4.05)	3.82(3.63)	8.01(8.25)	>350	68	751.05	1.87
$C_{39}H_{35}CuN_3O_{13}$/(HPC5)	57.13(57.32)	4.51(4.32)	5.38(5.14)	7.56(7.78)	>350	65	762.15	1.83
$C_{39}H_{33}CuN_3O_{12}$/(HPC6)	58.40(58.61)	3.94(4.16)	5.47(5.26)	7.73(7.95)	>350	60	762.42	1.86

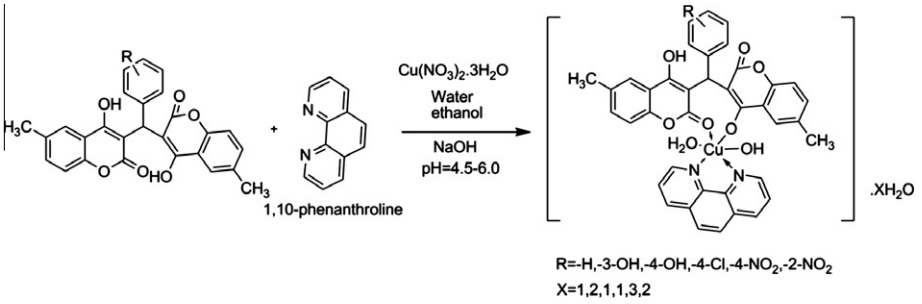

Scheme 2. General synthetic route of complexes (HPC).

Table 2
Antimicrobial and antioxidant activities of compounds.

Entry	Antimicrobial activity (minimal inhibition concentration)						Antioxidant activity
	Gram negative bacteria		Gram positive bacteria		Fungus		FRAP value (mmol/100 g)
	E. coli	*P. aeruginosa*	*S. pyogenes*	*B. subtilis*	*C. albicans*	*A. niger*	
HL1	400	400	100	70	200	200	NT
HL2	600	100	70	20	200	200	NT
HL3	400	100	40	20	200	200	NT
HL4	100	100	70	20	100	100	NT
HL5	200	200	70	70	200	200	NT
HL6	200	400	100	70	200	200	NT
HPC1	400	200	40	40	200	100	354
HPC2	600	100	20	20	200	200	405
HPC3	400	100	20	20	100	100	438
HPC4	70	100	40	20	100	100	402
HPC5	100	100	70	40	200	200	397
HPC6	200	200	70	40	200	200	377
Ciprofloxacin	20	10	20	05	NT	NT	NT
Norfloxacin	10	10	10	10	NT	NT	NT
Flucanazole	NT	NT	NT	NT	10	10	NT
Nystatin	NT	NT	NT	NT	100	100	NT
Ascorbic acid	NT	NT	NT	NT	NT	NT	–

E. Coli = ATCC25922; *P. aeruginosa* = ATCC25619; *S. pyogenes* = ATCC12384; *B. subtilis* = ATCC11774; *C. albicans* = ATCC 66027; *A. niger* = ATCC 64958.
NT = Not tested.

Table 3
Anti-tuberculosis activity of compounds.

Entry	MIC μg/mL *M. tuberculosis* (MTCC 200)	% Inhibition
HL1	50	35
HL2	12.5	36
HL3	50	18
HL4	12.5	82
HL5	50	64
HL6	100	32
HPC1	25	53
HPC2	3.125	92
HPC3	25	40
HPC4	12.5	90
HPC5	25	87
HPC6	50	68
Streptomycin	6.25	98
Isoniazid	0.25	99
Ethambutol	3.125	99

Elemental analysis

Analytical and physicochemical data of the complexes are summarized in Table 1. Complexes are colored and stable in air. They are insoluble in water and in most organic solvents but partially soluble in DMSO. The structure of the complexes is assumed according to the chemical reaction as shown below;

$$Cu(NO_3)_2 \cdot 3H_2O + HL + Ph \xrightarrow{dil.NaOH} [Cu(HL)(Ph)(H_2O)(OH)] \cdot XH_2O + 2NaNO_3 + XH_2O$$

where HL = HL1, HL2, HL3, HL4, HL5, HL6 (X = 1, 2, 1, 1, 3, 2).

IR spectra

The important infrared spectral bands and their tentative assignments for the synthesized compounds were recorded as KBr disks and are summarized in Table 4. The IR data of free ligands and its metal complexes were carried out within the IR range 4000–400 cm^{-1}. The IR spectra of the dicoumarol derivatives show weak bands at ~3135 cm^{-1}, ~3050 cm^{-1} and ~1330 cm^{-1}, ~1310 cm^{-1} corresponding to ν(O—H) respectively [36,37]. On complexation O—H peak has vanished indicates deprotonation of O—H proton. The ν(C=O) of lactone rings observed at ~1665 cm^{-1} in free ligand is shifted to lower frequencies (~15 cm^{-1}) due to complex formation [38], and further supported by shifting of ν(C—C), ν(C—O), and ν(C—O—C) stretch frequencies to higher values [39–41]. In IR spectrum of ligands and its complexes exhibited characteristic absorption band at ~2920 and at 2850–2700 cm^{-1} (asym. & sym. str.) for $\nu(CH_3)$ cm^{-1} and ~1450 cm^{-1} and ~1345 for (asym. & sym. str. of $\delta(CH_3)$ cm^{-1}). Two bands at ~1620 and ~1570 cm^{-1} were assigned to stretching vibration of conjugate double bonding in the free ligand [42]. The H—O—H bending mode occurring about 1600 cm^{-1} has not been observed because of the presence of strong absorbing group like methine group (—CH=). It is difficult to resolve both these bands [43]. A broad band at ~3430 cm^{-1} observed in the complex was due to the ν (OH) characteristic peak of a coordinated water molecule [44]. The IR spectrum of the free ligand shows a very stronger bands at ~1630 and ~1576 cm^{-1} due to stretching frequency of C=N present in 1,10-phenanthroline moiety. These bands were shifted to lower frequencies in the complexes ~30 cm^{-1}, which clearly indicate that it

Table 4
FT-IR data of synthesized compounds.

Complexes (HPC1–HPC6)	ν(OH/H_2O) cm^{-1}	ν(C=N) ^{w} cm^{-1}	ν(C=O) cm^{-1}	ν(C=C) cm^{-1}	ν(C—C) ν (C—O), ν (C—O—C) cm^{-1}	$\nu(CH_3)$ cm^{-1}	$\delta(CH_3)$ cm^{-1}	ν(Cu—N)^{w} cm^{-1}	ν(Cu—O)^{w} cm^{-1}
HPC1	3430(br)	1542	1652	1610	1182.1143, 1120, 852, 815, 782	2924(asy), 2862(sy)	1425(asy), 1343(sy)	465	565
HPC2	3428(br)	1544	1655	1613	1189, 1147, 1121.849, 816, 781	2923(asy), 2860(sy)	1428(asy), 1345(sy)	478	567
HPC3	3435(br)	1540	1650	1607	1185, 1138, 1120, 834, 818, 779	2925(asy), 2858(sy)	1432(asy), 1340(sy)	462	563
HPC4	3440(br)	1541	1647	1611	1186, 1141, 1123, 839, 820, 783	2923(asy), 2861(sy)	1425(asy), 1345(sy)	467	561
HPC5	3425(br)	1545	1645	1612	1188, 1142, 1126, 830, 824, 786	2927(asy), 2858(sy)	1432(asy), 1352(sy)	464	569
HPC6	3432(br)	1547	1653	1608	1180, 1149, 1127, 836, 827, 781	2931(asy), 2869(sy)	1435(asy), 1360(sy)	475	560

s = strong, w = weak, br = broad.

has been affected upon complexation via metal ions. In IR spectrum all the complexes shows the bands at ~549 and ~460 cm^{-1} due to the Cu—O and Cu—N respectively. Mehmet et al. mentioned the weak band around ~550 cm^{-1} and ~468 cm^{-1} were attributed to the Cu—O and Cu—N stretching frequency [45–47].

Mass spectra

The mass spectra of the complex **HPC1** ($C_{39}H_{32}CuN_2O_9$) reveals that molecular ion peak at *m/z* 717 of complex (without water of crystallization) along with several other peaks observed at 700, 682, 667, 652, 626, 574, 548, 471, 419, 367, 235, 207 and 117 *m/z* value.

Thermal studies

Each compound **(HPC1–HPC6)** has followed the decomposition process as shown below;

$$\text{Solid-1} \xrightarrow{\text{heat}} \text{Solid-2} + \text{Gas}$$

This process comprises several stages. The method reported by Freeman and Carroll [48] integral method of Coats and Redfern [49], the approximation method of Horowitz and Metzger [49] has been assumed. Plots of [$\Delta \log(dw/dt)/\Delta \log wr$] vs. [$\Delta(1/T)/\Delta \log wr$] were linear for all of the decomposition steps. The energy of activation E_a was calculated from the slopes of these plots for all stages and the order of reactions (n) determined from the intercept, showing first order reaction over the entire range of decomposition for all of the complexes. A typical plot for the thermal degradation of **HPC1** is shown in Fig. 1. All the complexes have negative entropy according to the kinetic data obtained from DTG curves, which specify that the synthesized complexes have higher controlled systems than reactants and are stable [49].

The thermal behavior of Cu(II) complexes

The thermal decomposition data of all the complexes are summarized in Tables 5 and 6. Thermogravimetric analysis (TG and DTG) representative curves corresponding to the complex **(HPC1)** are presented in Figs. 2 and 3, respectively. The thermal fragmentation scheme for the complexes is shown below;

$$[Cu(HL1)(Ph)(OH)(H_2O)]\cdot H_2O \xrightarrow[\text{Removal of one mole lattice water molecules}]{50-110\,^{\circ}C} [Cu(HL1)(Ph)(OH)(H_2O)] + H_2O$$

$$[Cu(HL1)(Ph)(OH)(H_2O)] \xrightarrow[\text{Removal of one mole ph ligand,—OH and } H_2O]{160-460\,^{\circ}C} [Cu(HL1)] + OH + H_2O + Ph$$

$$Cu(HL1)] \xrightarrow[\text{Removal of HL1ligand molecules}]{460-800\,^{\circ}C} \text{metal residue(CuO)} + HL1$$

The thermal decomposition occurs in three steps. In first step, endothermic decomposition between 50 and 110 °C attributed to dehydration process, which is due to loss of lattice water molecule. The mass loss observed is 2.82%, which is nearly equal to calculated value 2.51%. The loss of lattice water molecules is a first order and the value of the energy of activation for the dehydration process is found to be 3.58 kJ mol^{-1}. In the second step, endothermic decomposition between 160 and 460 °C corresponds to loss of coordinated water molecule, hydroxyl ion and 1,10-phenanthroline ligand. The observed mass loss is 32.01%, which is nearly equal to calculated value 29.99%. Next step, exothermic decomposition between 460 and 800 °C corresponds to loss of coordinated **HL1** ligand. The observed mass loss is 38.59%.

First is dehydration process with endothermic effect on DTG curve at 108 °C, while increasing in temperature of [Cu(HL1)(Ph)(H_2O)(OH)], which shows also endothermic effect at 290 °C respectively. Exothermic DTG peak at 487 °C associated with elimination of **HL1** ligand.

In our investigation, thermal behaviors of the all complexes in terms of stability, peak temperatures and values of kinetic parameters are calculated. Kinetic parameters of decomposition method such as entropy (S^*), enthalpy (H^*), pre-exponential factor (A), and Gibbs free energy of the decomposition (G^*), were studied using the Horowitz–Metzger equation method is discussed in brief and the results obtained by these methods are well correlated with each other and summarized in Table 6. The pre-exponential factor, A, was calculated from the equation: $E_a/RTs^2 = A/\Phi \exp(-E_a/RTs)$. The entropy ($S^*$), enthalpy ($H^*$), and Gibbs free energy, (G^*), were calculated from: $S^* = 2.303(\log Ah/KTs)\ R$, $H^* = E_a - RTs^*$ *and* $G^* = H^* - Ts\ S^*$ respectively. Where h is the Plank constant, Φ is the heating rate, K is the Boltzmann constant, and Ts is the temperature of peak from DTG curve. According to the kinetic data obtained from DTG curves, all the complexes have negative entropy, which indicates that the studied complexes have more ordered systems [50]. The energy of activation (E_a) is helpful in assigning the strength of the bonding of ligand moieties with the metal ion. The relative high E_a value (Table 6) indicates that both the ligands is strongly bonded to the metal ion [51].

Reflectance spectra and magnetic measurement

The information regarding geometry of the mixed-ligand complexes has been obtained from their electronic spectral data along with magnetic susceptibility measurements. Cu(II) complexes (d^9 system) are known for their varieties of structures due to their various coordination numbers. Six-coordinated Cu(II) complexes possesses distorted octahedral geometry. Normal octahedral geometry

was found for Cu(II) complexes [52,53], even though the known preference for Jahn–Teller distortions in cases of trigonal and octahedral geometry. A very weak low intensity absorption band associated with d–d transition for Cu(II) complexes at 465, 532 nm was typical octahedral transition its indicate the octahedral geometry of complexes [54]. moreover, the electronic spectra of six coordinate Cu(II) complexes have either D4h or C4v symmetry, and the Eg and T2g level of the 2D free ion term will split into B1g, A1g, B2g and Eg levels, respectively under the influence of the distortion, which can be cause two transitions such as, 2B1g → 2B2g and 2B1g → 2A1g. This supports the distorted octahedral Cu(II) complex which is usual in the d9 system [55,56]. The electronic spectra of Cu(II) complexes **(HPC1–HPC6)** show three important bands. Low intensity broad band in the region ~18,000 cm^{-1} is assigned as 10 Dq band corresponding to 2Eg → 2T2g transition [57]. There is a high intensity band in the region ~24,000 cm^{-1} due to symmetry forbidden ligand → metal charge transfer transition [58]. The band above 27,000 cm^{-1} is assigned as ligand band. Therefore distorted octahedral geometry around Cu(II) ion is suggested on the basis of electronic spectra [59], which is further ascertain by its magnetic moment of the Cu(II) complexes lies in between 1.82 and 1.96 BM range. These values are typical of mononuclear Cu(II) compounds with d^9 electronic configuration. The observed magnetic moments of all complexes correspond to characteristic high-spin octahedral complexes. However, these values are slightly higher than the expected spin-only values due to spin–orbit coupling contribution [60]. Thus the electronic spectral data and magnetic moment data support the octahedral geometry of the all complexes.

X-ray diffraction studies

X-ray powder diffraction studies is carried out two find the feasible lattice dynamics of the finely powdered compound **HPC2** (Fig. 4). The observed inter planar spacing values (d-spacing) were measured from the diffractogram of the compound. Furthermore, the Miller indices *h*, *k* and *l* were assigned to each d value along with 2-Theta angles are given in Table 7. The results show that the compound belongs to hexagonal crystal system having unit cell parameters as *a* = 4.9168, *b* = 4.9168, *c* = 5.4089, maximum deviation of 2-Theta = 0.025 and Alpha = 90, Beta = 90, Gama = 120 at the wavelength = 1.540598. We have tried to isolate single crystal of Cu(II) complex for accurate X-ray crystal study but could not succeed to develop single crystal, it might be due to polycrystalline nature of complex. It is difficult to grow good quality single crystals of entitled Cu(II) complexes. In such cases, the powder X-ray diffraction studies might be useful. Even with some inherent limitations, this method yield valuable information about the characteristics of the crystal w3x. Yang and Dang [61] were recently reported the X-ray powder diffraction studies for structure of hexa-coordinated Tin(IV) complex in which the ligand adopts the most stereo-chemically favorable orientation. On the basis of the X-ray powder diffraction study, proposed structure as per Fig. 5 suggested for the complexes.

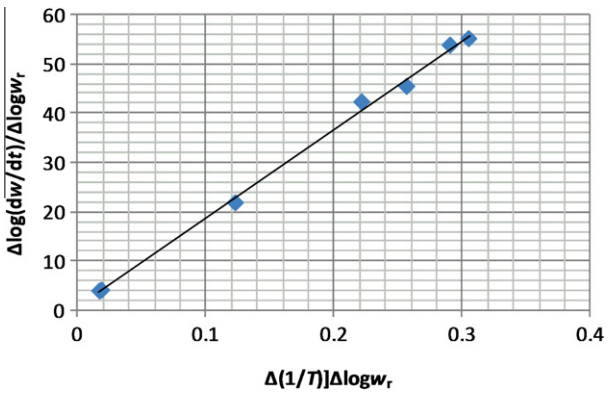

Fig. 1. Thermal degradation of HPC1.

Antimicrobial

The examination of the data (Table 2) revealed that majority of the compounds showed good antibacterial and antifungal activity when compared with standard drugs. Transition metal complexes posses higher antimicrobial activity compared to the coumarin derivatives may be due to the change in structure by coordination and chelating tends to make metal complexes act as more powerful and potent bactereostatic agents, thus inhibiting the growth of the microorganisms [62,63]. According to which the polarities of the ligands and the central metal atoms are reduced through charge equilibration over the whole chelate ring. The process turns that increase the lipophilic character of the central metal atom which favors its permeation through the lipid layer of the microorganism and thus destroying them more aggressively. As shown in Table 2, Complexes **HPC2**, **HPC3** and **HPC4** were found to be higher potency against most of the employed strains. In particular, against Gram Positive bacteria *S. Pyogenes*, complexes **HPC2** and **HPC3** have shown superior activity upon comparison with standard drugs. Unfortunately, none of the synthesized ligands and its transition metal complexes were found sufficiently potent to inhibit Gram negative bacteria. Furthermore, against fungal pathogen *A. niger*, complex **HPC1** showed significant activity. While, ligand **HL4** and complexes **HPC3** as well as **HPC4** displayed excellent activity upon comparison with Nystatin against both fungal pathogen.

The investigation of the structure–activity relationship of antibacterial screening revealed that the ligand **HL1** was found to have activity (MIC = 400 μg/mL) towards *P. aeruginosa*, (MIC = 100 μg/mL) towards *S. pyogenes*, (MIC = 70 μg/mL) towards *B. subtilis* and (MIC = 200 μg/mL) towards *A. niger* but after formation of complex with Cu(II), resulted complex **HPC1** have been found to posses increased the potency (MIC = 200 μg/mL) against *P. aeruginosa*, (MIC = 40 μg/mL) against *S. pyogenes*, (MIC = 40 μg/mL) against *B. subtilis* and (MIC = 100 μg/mL) against *A. niger*. Same thing is observed in case of ligand **HL5** have shown activity (MIC = 200 μg/mL) against *E. coli*, (MIC = 200 μg/mL) against *P. aeruginosa* and (MIC = 70 μg/mL) against *B. subtilis* but after formation of complex with Cu(II), resulted increase the potency of complex **HPC5** towards *E. coli* (MIC = 100 μg/mL), towards *P. aeruginosa* (MIC = 100 μg/mL) and towards *B. subtilis* (MIC = 40 μg/mL).

Moreover, complex **HPC2** having *m*-hydroxy phenyl ring at 3-position of coumarine nucleus have been found inactive against *E. coli*, *C. albicans* and *A. niger* but changing the position of hydroxyl group to *p*-position of phenyl ring (complex **HPC3**), resulted increase the activity towards *E. coli*, *C. albicans* and *A. niger*. Similar situation observed in case of complex **HPC6** carrying o-nitro phenyl ring at 3-position of coumarine moiety showed inactivity against gram negative bacteria *E. coli* and *P. aeruginosa*, while replacing the o-position of nitro group to *p*-position of phenyl ring(complex **HPC5**), resulted increase the antibacterial potency towards *E. coli* and *P. aeruginosa*.

Interestingly, the complexes **HPC3**, **HPC4** and **HPC5** with substitutions at *p*-position of the phenyl ring displayed good inhibitory action against most of the employed strains than (un)substitutions at other position of phenyl ring as well as ligand **HL4** and its complex **HPC4** carrying chloro substitution at *p*-position of the phenyl ring showed better activity against both fungal pathogen. Complexes **HPC2** and **HPC3** have been found chief antimicrobial members against gram positive bacteria.

Table 5
Thermoanalytical data of Cu(II) complexes.

Complexes	TG range (°C)	DTG_{max} (°C)	Mass loss (% obs. (calcd.))	Assignment
$[Cu(HL1)(Ph)(H_2O)(OH)]H_2O$	50–110	108	2.82(2.51)	Removal of one mole lattice H_2O molecule
	160–460	290	32.01(29.99)	Removal of one mole Ph ligand, —OH and H_2O
	460–800	487	38.59	Removal of HL1 ligand
$[Cu(HL2)(Ph)(H_2O)(OH)]2H_2O$	60–110	102	4.64(4.91)	Removal of two mole lattice H_2O molecule
	180–450	294	30.69(29.33)	Removal of one mole Ph ligand, —OH and H_2O
	450–800	479	43.20	Removal of HL2 ligand
$[Cu(HL3)(Ph)(H_2O)(OH)]H_2O$	50–100	82	2.94(2.45)	Removal of one mole lattice H_2O molecule
	160–450	284	31.49(29.33)	Removal of one mole Ph ligand, —OH and H_2O
	450–800	498	45.23	Removal of HL3 ligand
$[Cu(HL4)(Ph)(H_2O)(OH)]H_2O$	70–130	97	2.67(2.39)	Removal of one mole lattice H_2O molecule
	170–480	280	28.32(28.63)	Removal of one mole Ph ligand, —OH and H_2O
	480–800	471	52.36	Removal of HL4 ligand
$[Cu(HL5)(Ph)(H_2O)(OH)]3H_2O$	40–100	89	7.52(7.08)	Removal of three mole lattice H_2O molecule
	160–470	297	29.85(28.22)	Removal of one mole Ph ligand, —OH and H_2O
	470–800	490	49.23	Removal of HL5 ligand
$[Cu(HL6)(Ph)(H_2O)(OH)]2H_2O$	70–150	120	4.29(4.72)	Removal of two mole lattice H_2O molecule
	190–510	288	28.63(28.22)	Removal of one mole Ph ligand, —OH and H_2O
	510–800	497	44.32	Removal of HL6 ligand

Table 6
Kinetic parameters of Cu(II) complexes.

Complex	TG range (°C)	E_a (kJ mol^{-1})	n	A (s^{-1})	S^* (J K^{-1} mol^{-1})	H^* (kJ mol^{-1})	G^* (kJ mol^{-1})
$[Cu(HL1)(Ph)(H_2O)(OH)]H_2O$	50–110	3.58	1.30	0.108	−102.45	0.576	37.66
	160–460	3.67	1.32	0.062	−101.06	0.021	45.36
	460–800	39.35	1.00	6.48	−97.37	31.26	126.01
$[Cu(HL2)(Ph)(H_2O)(OH)]2H_2O$	60–110	3.76	1.42	0.127	−105.59	0.541	35.85
	180–450	6.31	1.12	0.037	−102.36	0.054	43.47
	450–800	42.57	1.37	5.83	−94.32	34.78	135.56
$[Cu(HL3)(Ph)(H_2O)(OH)]2H_2O$	50–100	3.87	1.07	0.185	−101.04	0.743	39.77
	160–450	4.23	1.27	0.023	−98.18	0.86	42.18
	450–800	51.26	1.52	7.54	−93.27	39.82	142.48
$[Cu(HL4)(Ph)(H_2O)(OH)]H_2O$	70–130	3.78	1.39	0.165	−109.72	0.876	36.45
	170–480	9.45	1.35	0.071	−95.62	0.073	52.16
	480–800	47.29	1.12	4.67	−92.37	41.31	123.92
$[Cu(HL5)(Ph)(H_2O)(OH)]3H_2O$	40–100	3.35	0.98	0.147	−104.25	0.593	33.73
	160–470	6.57	1.23	0.065	−103.37	0.062	48.56
	470–800	53.78	1.03	6.54	−90.46	38.54	127.47
$[Cu(HL6)(Ph)(H_2O)(OH)]2H_2O$	70–150	3.56	1.12	0.173	−103.82	0.485	38.46
	190–510	7.82	1.41	0.035	−97.32	0.035	44.76
	510–800	49.17	1.08	7.78	−94.63	40.68	122.35

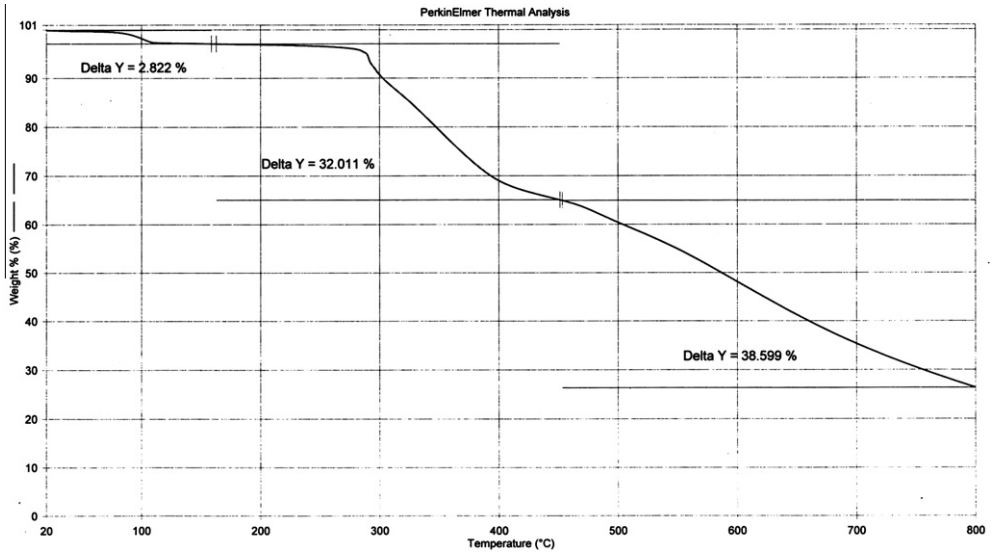

Fig. 2. TG curve of HPC1.

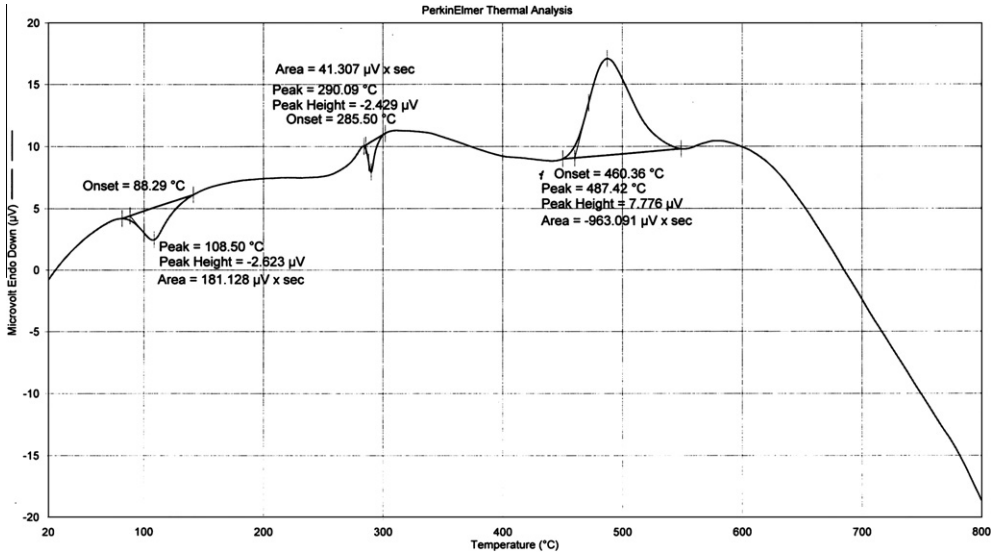

Fig. 3. DTG curve of HPC1.

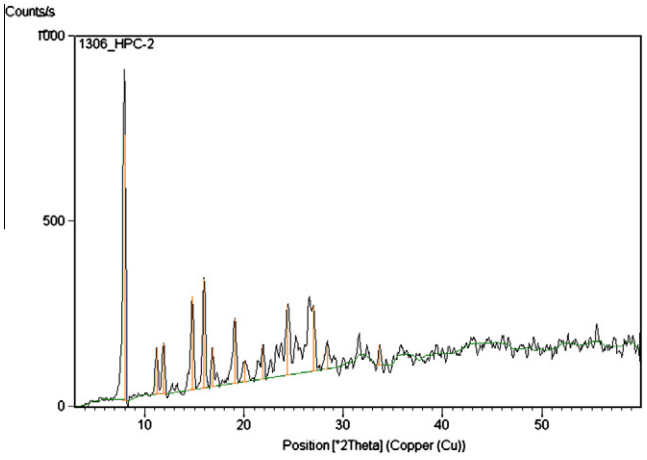

Fig. 4. XRD pattern of HPC2.

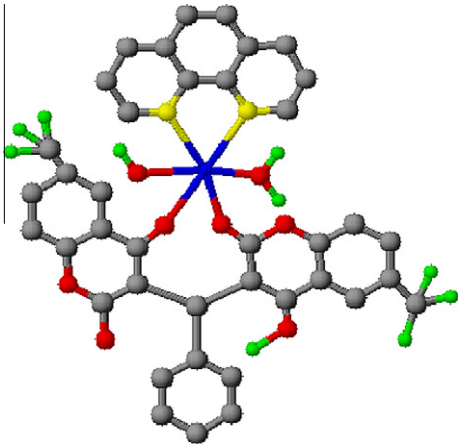

Fig. 5. Proposed 3D structure of complex.

Reviewing and comparing the activity data, it is worthy to mention that the antimicrobial activity of the target complexes depends not only on the bicyclic heteroaromatic pharmacophore appended through aryl ring but also on the nature of the metal coordinated with ligands.

Antioxidant

In vitro antioxidant activity of all the complexes **HPC1–HPC6** is shown in Table 2, exposed moderate to good ferric reducing power. Among the tested compound, **HPC3** showed more potency (FRAP value 438 mM/100 g of sample), while **HPC1** have less Frap value (354 mM/100 g of sample). Furthermore, obtained data revealed that hydroxyl group substituted derivatives show more ferric reducing power compared to that of chloro, nitro or unsubstituted one. Thus form the data obtained, the potency order on the basis of various substitutions on 4-position of the phenyl ring is given as —OH > —Cl > —NO_2 > —H. However, none of the compounds have been found to show better activity compared to the standard ascorbic acid.

Anti-tubercular activity

The anti-tubercular activities of all the synthesized ligand and its complexes were assessed against *M. tuberculosis* H37Rv at different concentration 3.125, 6.25, 12.5, 25, 50 and 100 µg/mL. The Minimum Inhibitory Concentrations (MICs) of test compounds compared with standard drugs Isoniazid, Ethambutol and

Table 7
Observed and calculated X-ray diffraction data of [Cu(HL2)(Ph)(H_2O)(OH)]·2H_2O complex.

h	*k*	*l*	2Theta (Obs.)	2Theta (Calc.)	2Theta (Diff.)	*d* (Obs.)	*d* (Calc.)	*d* (Diff.)	Intensity (Obs.)
0	0	1	16.8028	16.375	0.4278	5.27652	5.40890	−0.13238	10.46
1	0	0	20.0306	20.845	−0.8144	4.43294	4.25807	0.17487	10.93
1	0	1	26.9808	26.622	0.3588	3.30473	3.34573	−0.041	20.81
0	0	2	33.6646	33.097	0.5676	2.66234	2.70445	−0.04211	7.67

Streptomycin as well as % inhibition are summarized in (Table 3). From the compounds screened for anti-tuberculosis activity, ligands show inhibition concentrations at 100 μg/mL and 50 μg/mL except **HL2**, **HL4** at 12.5 μg/mL. A complex **HPC6** also exhibits activity at 50 μg/mL concentration while **HPC2** and **HPC4** complexes have found to possess better activity with MIC of 3.125 μg/mL and 12.5 μg/mL along with inhibition of 92% and 90% respectively, where other complexes exhibits MIC at 25 μg/mL. Compound **HPC2** has been emerged as the promising anti-tubercular member due to better activity along with compared to Streptomycin.

Conclusions

The synthesized Cu(II) complexes are confirmed based on data obtained from physico-chemical, spectroscopic, X-ray diffraction, magnetic and thermal properties . The coordination ability of the ligands has been proved in complexation reaction with Cu(II) ion. Structures for all metal complexes suggested coordination of the ligands through both the hydroxyl and carbonyl oxygen atoms. Thermal studies (TG and DTG) carried out for Cu(II) complexes show presence of lattice water molecules in respective compounds. TG curves of complexes shows weight loss of 32.01% in temperature range 160–460 °C may be assigned to coordinated Ph legends, hydroxyl ion and water molecule. X-ray diffraction results show that the compound belongs to hexagonal crystal system with polycrystalline nature of complex which was suggested octahedral geometry. Further the geometry was confirmed using electronic spectra and magnetic moment value. The kinetic parameters calculated by Freeman–Carroll method, especially activation energy (E_a), are useful in assigning the strength of the complexes. Result from Antimicrobial activity, the comparative study between ligands and their complexes showed the increase in the activity of complexes than ligands due to their coordination to the metal. *In vitro* anti-tubercular activity of all synthesized compounds shows good results with an enhancement of activity on complexation among metal ions. Especially complexes **HPC2** has been emerged as the promising anti-tubercular member due to excellent activity along with compared to Streptomycin, while good antioxidant power was shown by complexes as compared to ascorbic acid.

Acknowledgements

Authors are grateful to The Principal, and management of V. P. & R. P. T. P. Science College, Sardar Patel University, Vallabh Vidyanagar for providing Research facilities. Authors are thankful to The Director, SICART, Vallabh Vidyanagar for X-ray diffraction, FT-IR and electronic spectral analysis facility. We are articulate our appreciation to IIT-Bombay for TG and DTG scan analysis facility. Authors are also grateful to The Director, SAIF-RSIC, Panjab University, Chandigarh for NMR analysis and Central Diagnostic Laboratory for providing biological analysis facilities.

Appendix A. Supplementary material

Supplementary data associated with this article can be found, in the online version, at http://dx.doi.org/10.1016/j.saa.2012.09.096.

References

[1] O. Zaneva, I. Manolov, N. Danchev, Pharmacia, Sofia LII 1-2 (2005) 85–89.
[2] I. Manolov, C. Maichle-Moessmer, I. Nicolova, N. Danchev, Arch. Pharm. Chem. Life Sci. 339 (2006) 319–326.
[3] U.S. Steffen, B. Weber, C. Siegers, Res. Commun. Mol. Pathol. Pharmacol. 99 (1998) 193–206.
[4] H. Zhao, N. Neamati, H. Hong, A. Mazumder, S. Wang, S. Sunder, G.W. Miline, Y. Pommier, T.R. Burke, J. Med. Chem. 40 (1997) 242–249.
[5] P.C. MinMao, J.F. Mouscadet, H. Leh, C. Auclair, L.Y. Hsu, Chem. Pharm. Bull. 50 (2002) 1634–1637.
[6] C.X. Su, J.F. Mouscadet, C.C. Chiang, H.J. Tsai, L.Y. Hsu, Chem. Pharm. Bull. 54 (2006) 682–686.
[7] I. Kostova, S. Raleva, P. Genova, R. Argirova, Bio. Inorg. Chem. Appl. 2006 (2006) 1–9.
[8] C. Xin Zhang, S. Lippard, Curr. Opin. Chem. Biol. 7 (2003) 481–489.
[9] H. Sakurai, Y. Kojima, Y. Yoshikawa, K. Kawabe, H. Yasui, Coord. Chem. Rev. 226 (2002) 187–198.
[10] P.J. Sadler, H. Li, H. Sun, Coord. Chem. Rev. 185–186 (1999) 689–709.
[11] H. Ali, J.E. van Lier, Chem. Rev. 99 (1999) 2379–2450.
[12] A.Y. Louie, T.J. Meade, Chem. Rev. 99 (1999) 2711–2734.
[13] W.A. Volkert, T.J. Hoffman, Chem. Rev. 99 (1999) 2269–2292.
[14] P.G. Sammes, G. Yahioglu, Chem. Soc. Rev. 23 (1994) 327–334.
[15] C.R. Luman, F.N. Castellano, in: J.A. McCleverty, T.J. Meyer, A.B.P. Lever (Eds.), Comprehensive Coordination Chemistry, vol. 1, Elsevier, Oxford, UK, 2004, p. 25.
[16] S.F. Ashcroft, C.T. Mortimer, Thermochemistry of Transition Metal Complexes, Academic Press, NY, USA, 1970;
S.J. Ashcroft, C.T. Mortimer, Thermochemistry of Transition Metal Complexes, Academic Press, London, 1970. pp. 233–237, 384–391.
[17] G. Anderegg, Helv. Chim. Acta 46 (1963) 2397–2410.
[18] G. Anderegg, Helv. Chim. Acta 46 (1963) 2813–2822.
[19] R. Olar, M. Badea, O. Carp, D. Marinescu, V. Veronica Lazar, C. Balotescu, A. Dumbrava, J. Therm. Anal. Calorim. 92 (2008) 245–251.
[20] J. Al-Enfermo, Enferm Infecc Microbiol Clin. 21 (2003) 261–267.
[21] L. Jia, P. Jiang, J. Xu, Z. Hao, X. Xu, L. Chen, J. Wu, N. Tang, Q. Wang, J.J. Vittal, Inorg. Chim. Acta 363 (2010) 855–865.
[22] G.J. Kharadi, K.D. Patel, J. Therm. Anal. Calorim. 96 (2009) 1019–1028.
[23] G.J. Kharadi, K.D. Patel, Appl. Organomet. Chem. 23 (2009) 391–397.
[24] K.S. Patel, J.C. Patel, H.R. Dholariya, Spectrochim. Acta Part A. 96 (2012) 468–479.
[25] J.C. Patel, H.R. Dholariya, K.S. Patel, K.D. Patel, Appl. Organomet. Chem. <http://www.dx.doi.org/10.1002/aoc.2907>.
[26] C.L. Albano, R. Sciamanna, T. Aquino, J.J. Martinez, European Congress on Computational Methods in Applied Sciences and Engineering, ECOMAS, Barcelona, 2000.
[27] F. Carrasco, Thermochim. Acta 213 (1993) 115–134.
[28] A.I. Vogel, Textbook of Practical Organic Chemistry, fifth ed., Longman, London, 1989.
[29] F.E. Mabbs, D.I. Machin, Magnetism and Transition Metal Complexes, Chapman and Hall, London, 1973.
[30] J.L. Bose, V.R. Shah, R.C. Shah, J. Org. Chem. 25 (1960) 677–679.
[31] Clinical and Laboratory Standards Institute (CLSI) (formerly NCCLS), Performance Standards for Antimicrobial Disk Susceptibility Tests, Approved Standard, M2-A9, Clinical and Laboratory, Standards Institute, 940 West Valley Road, Wayne, Pennsylvania, USA, 2006.
[32] N. Parmar, S. Teraiya, R. Patel, H. Barad, H. Jajda, V. Thakkar, J. Saudi Chem. Soc. 1 (2012) 1–2. http://dx.doi.org/10.1016/j.jscs.2011.12.014.
[33] J.M. Andrew, J. Antimicrob. Chemother. 48 (2001) 563–567.
[34] A. Rattan, in: B.I. Churchill (Ed.), Antimicrobials in Laboratory Medicine, Livingstone, New Delhi, 2000, pp. 85–108.
[35] T.N. Akhaja, J.P. Raval, Eur. J. Med. Chem. 46 (2011) 5573–5579.
[36] I. Kostova, G. Momekov, M. Zaharieva, M. Karaivanova, Eur. J. Med. Chem. 40 (2005) 542–551.
[37] T.M.A. Ismail, J. Coord. Chem. 58 (2005) 141–151.
[38] N.B. Patel, G.P. Patel, J.D. Joshi, J. Macro. Mol. Sci. 42 (2005) 931–943.
[39] A.O. Görgülü, M. Arslan, E. Cil, J. Coord. Chem. 58 (2005) 1225–1231.
[40] R.C. Paul, S.L. Chadha, Indian J. Chem. 8 (1970) 739.
[41] F.D. Lewis, S.V. Barancyk, J. Am. Chem. Soc. 111 (1989) 8653–8661.
[42] R.M. Silverstein, F.X. Webster, Spectrometric Identification of Organic Compounds, sixth ed., John Wiley & Sons, New York, 2004.
[43] P.B. Pansuriya, M.N. Patel, Appl. Organometal. Chem. 21 (2007) 719–727.
[44] L.N. Sharada, M.C. Ganorkar, Indian J. Chem. 27 (1988) 542–544.
[45] F. Karipcin, E. Kabalcilar, Acta. Chim. Slov. 54 (2007) 242–247.
[46] T. Mehmet, K. Huseyin, S. Selhattin, Trans. Met. Chem. 24 (1999) 13–17.
[47] S. Chandra, L.K. Gupta, Spectrochim. Acta Part A 61 (2005) 269–275.
[48] E.S. Freeman, B. Carroll, J. Phys. Chem. 62 (1958) 394–397.
[49] M.S. Refat, S.A. El-Korashy, A.S. Ahmed, Spectrochim Acta part A. 71 (2008) 1084–1094.
[50] C.K. Modi, M.N. Patel, J. Therm. Anal. Cal. 94 (2008) 247–255.
[51] M.E. El-Zaria, Spectrochim. Acta Part A 69 (2008) 216–221.
[52] W.N. Setzer, C.A. Ogle, G.S. Wilson, R.S. Glass, Inorg. Chem. 22 (1983) 266–271.
[53] H. Olmez, F. Arslan, H. Icbud, J. Therm. Anal. Calorim. 76 (2004) 793–800.
[54] A.A. Ahmed, S.A. BenGuzzi, A.A. Hadi, J. Sci. Appl. 1 (2007) 79–90.
[55] M.V. Angelusiu, S.F. Barbuceanu, C. Draghici, G.L. Almajan, Eur. J. Med. Chem. 45 (2010) 2055–2062.
[56] V.P. Singh, A. Katiyar, Pestic. Biochem. Physiol. 92 (2008) 8–14.
[57] K.C. Patel, D.E. Goldberg, J. Inorg. Nucl. Chem. 34 (1972) 637–649.
[58] A.L. Abuhijleh, C. Woods, I.Y. Ahmed, Inorg. Chim. Acta 190 (1991) 11–17.
[59] D.P. Singh, R. Kumar, V. Malik, P. Tyagi, Trans. Met. Chem. 32 (2007) 1051–1055.
[60] F.A. Cotton, G. Wilkinson, Advanced Inorganic Chemistry, fifth ed., Wiley, New York, 1988.
[61] H.J. Yang, Y.Q. Dang, Acta Cryst. 65 (2009) 398–410.
[62] N. Raman, S.J. Raja, A. Sakthivel, J. Coord. Chem. 62 (2009) 691–709.
[63] R.S. Srivastava, Inorg. Chim. Acta 56 (1981) 165–168.